Structural and electronic properties of ZnO polycrystals doped with Co

2009 J. Phys.: Condens. Matter 21 064215

(http://iopscience.iop.org/0953-8984/21/6/064215)

J. Phys.: Condens. Matter **21** (2009) 064215 (5pp) doi:10.1088/0953-8984/21/6/064215

Structural and electronic properties of ZnO polycrystals doped with Co

N Hasuike[1], K Nishio[1], H Katoh[1], A Suzuki[1], T Isshiki[1], K Kisoda[2] and H Harima[1]

[1] Department of Electronics, Kyoto Institute of Technology, Kyoto 606-8585, Japan
[2] Department of Physics, Wakayama University, Wakayama 640-8510, Japan

E-mail: hasuike@kit.ac.jp

Received 28 June 2008, in final form 25 September 2008
Published 20 January 2009
Online at stacks.iop.org/JPhysCM/21/064215

Abstract

$Zn_{1-x}Co_xO$ samples were prepared by a standard solid-state reaction method. $Zn_{1-x}Co_xO$ crystals in the wurtzite structure were obtained with a Co composition of up to 22.1%. The a- and c-axis lengths increased and decreased, respectively, with an increase in Co composition. Raman spectra showed systematic broadening of the E_2 (high) phonon mode associated with the increase in Co composition, and electronic transitions of Co in the oxygen tetrahedron were observed in optical absorption measurement. These results indicated systematic substitution of Co into the Zn sites. Furthermore, an additional broad absorption band at 2.4–3.3 eV corresponding to the charge transfer (CT) process ($Co^{2+} \rightarrow Co^{1+}$) was also observed. The Raman spectra showed strong enhancement of the LO phonon due to a resonant Raman process induced with the coupling of the LO phonon and a photo-excited carriers mediated CT gap. These results suggest the possibility of carrier-induced ferromagnetism based on double exchange interaction in $Zn_{1-x}Co_xO$ by visible light irradiation.

1. Introduction

ZnO has attracted much attention for optoelectronic devices such as light emitting diodes working in the near ultraviolet region due to its wide direct band gap of 3.3 eV and large exciton binding energy of 60 meV. For a further industrial application, transparent conductive films have also been intensively studied as replacements for ITO conductive film.

More recently, ZnO doped with magnetic elements (DMS; diluted magnetic semiconductor) has attracted much attention for spintronics applications, because theoretical calculations predicted carrier-induced ferromagnetism above room temperature [1, 2]. According to a theoretical prediction, localized spins may be ferromagnetically coupled through interactions with free carrier spin. In this theoretical approach, however, high concentrations of magnetic elements and carriers were required at the same time.

Actually, many experiments have reported room temperature ferromagnetism in ZnO doped with 3d transition metals [3–11]. On the other hand, negative experimental aspects have been also reported that the ferromagnetism may derive from a phase-separated magnetic cluster [12] and samples have shown a paramagnetic behavior [13–16]. Hence, the mechanism of ferromagnetism is still under discussion.

Furthermore, there is also another theoretical prediction that the ferromagnetic ordering comes from the inhomogeneous distribution of magnetic elements in the host lattice [17]. According to this theoretical model, the inhomogeneous distribution of magnetic elements generates nanometer-sized clusters rich in magnetic elements as a spinodal decomposed phase, and a network of such clusters shows ferromagnetic ordering above room temperature. That is, macroscopic magnetic ordering is strongly correlated with the uniformity of magnetic elements.

As mentioned above, the magnetic properties in DMS are sensitively dependent on the sample quality. However, it is difficult to grow high-quality ZnO crystals uniformly doped with magnetic elements that are well controlled for the conductive type and carrier concentration. Therefore, the development of a growth technique for high-quality DMS crystals and the evaluation in detail of structural and electronic properties are required to investigate the mechanism of ferromagnetism.

In this work, we studied in detail the structural and electronic properties of ZnO doped with Co synthesized by a solid-state reaction.

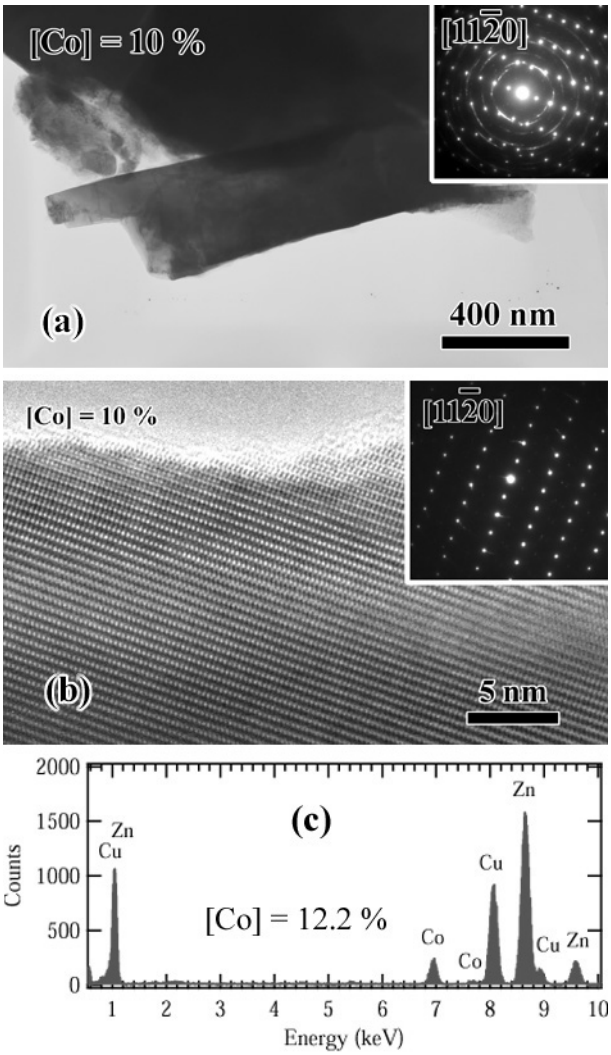

Figure 1. TEM image of the sample of [Co] = 10% in preparation recipe (a) and its magnified image (b), and their SAED patterns are shown in the insets. (c) The EDX spectrum taken from the area shown in (b).

2. Experimental details

$Zn_{1-x}Co_xO$ samples were prepared by a standard solid-state reaction method using commercially-supplied ZnO powder and metallic Co powder as starting materials. Mixtures of ZnO and Co powder were sintered in air at 1000 °C for 6 h. The composition of Co was varied at 0, 7, 10 and 20% in the preparation recipe.

The crystal structure and configuration of the samples were observed by x-ray diffraction (XRD), transmission electron microscopy (TEM) and selected area electron diffraction (SAED), and the sample composition was evaluated by energy dispersive x-ray (EDX) analysis. For optical characterization, Raman scattering was observed at room temperature by a confocal microscope using an Ar^+ laser at 457.9, 488.0 and 514.5 nm, and using a double monochromator equipped with a liquid-N_2-cooled CCD (charge coupled device) detector. Optical absorption measurements were also conducted at room temperature using a UV–visible–NIR spectrophotometer.

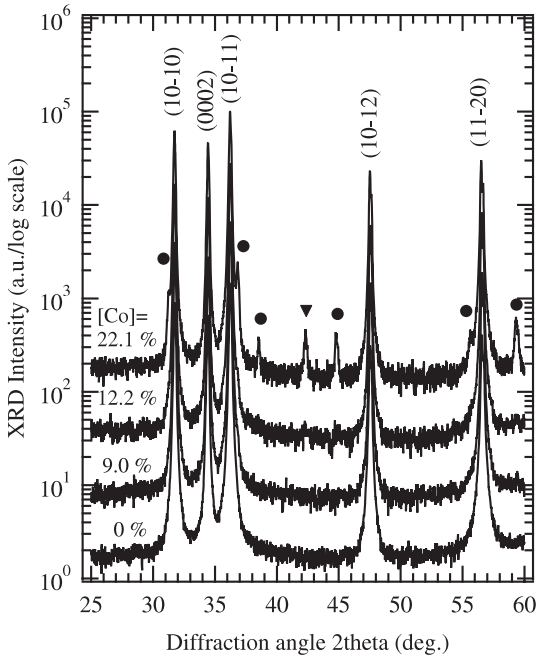

Figure 2. X-ray diffraction patterns for $Zn_{1-x}Co_xO$ samples. The Co composition is denoted in the figure. Filled circles and triangles correspond to Co_3O_4 and CoO, respectively.

3. Results and discussions

Figure 1(a) shows the TEM image for the sample with a composition of Co = 10%, and the inset shows its SAED pattern observed from the [11$\bar{2}$0] direction in the wurtzite structure. Also, figure 1(b) and its inset show the high-resolution TEM image and SAED pattern of the sample shown in figure 1(a). These results revealed that μm-sized crystals in wurtzite ZnO structure were synthesized, and the lattice fringe corresponding to Zn and O stacking layers in the [0001] direction was clearly observed.

The Co composition was analyzed by EDX analysis as shown in (c). The EDX spectrum was taken from the single crystal area in the wurtzite structure. The Cu signal is an artifact coming from the sample holder. The Co composition was estimated to be about 12.2% from the intensity ratio of Co and Zn signals. For other samples with [Co] = 7 and 20% in the preparation recipe, the Co composition was also estimated to be about 9.0 and 22.1%, respectively.

Figure 2 shows XRD patterns for all the samples. Clear XRD patterns corresponding to a wurtzite ZnO structure were observed. For the sample of [Co] = 22.1%, however, impurity phases corresponding to Co_3O_4 and CoO were observed, as marked by filled circles and triangles respectively. With an increase in Co composition, the (0002) and (11$\bar{2}$0) diffraction peak shifts lightly to the higher and lower angles as shown in figures 3(a) and (b), indicating that the *a*- and *c*-axis lengths slightly increased and decreased, as shown in figure 3(c), respectively [3].

Figure 4 shows optical absorption spectra for all the samples. The sample with [Co] = 0% (undoped) shows a clear band edge absorption at 3.3 eV. On the other hand, feature

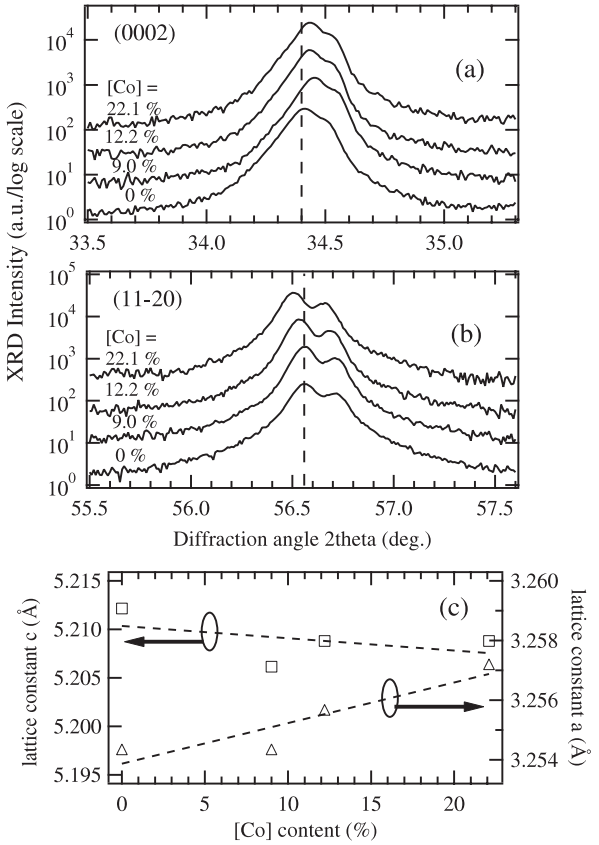

Figure 3. The close-up of (0002) (a) and (11$\bar{2}$0) (b) diffraction peak. The dependence of *a*- and *c*-axis lengths on Co composition (c).

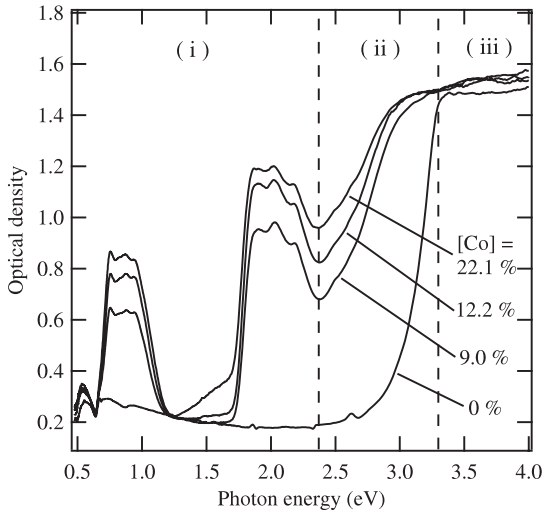

Figure 4. Optical absorption spectra for the $Zn_{1-x}Co_xO$ samples. Three regions denoted by (i), (ii) and (iii) correspond to the electronic transition of Co 3d orbitals, the charge transfer gap and the band gap of the ZnO host lattice, respectively.

absorption bands at ∼0.8, ∼2.0 eV were observed for the samples doped with Co. They correspond to the electronic transition of Co 3d orbitals in the oxygen tetrahedron [18, 19], showing the incorporation of Co into the Zn sites in the wurtzite ZnO host lattice. Furthermore, an additional broad

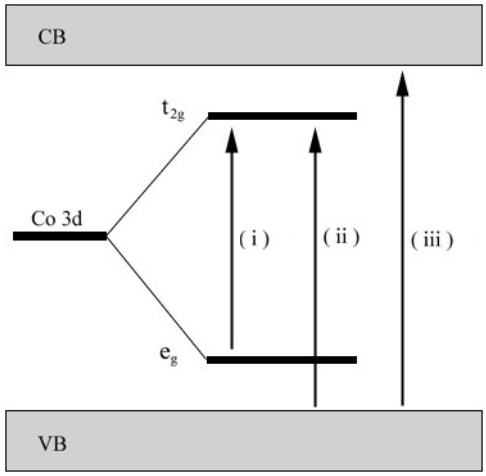

Figure 5. The energy band diagram of ZnO doped with Co. Characteristic transitions denoted by (i), (ii) and (iii) correspond to feature absorptions in the optical absorption spectra.

absorption band at 2.4–3.3 eV was also observed. This broad absorption band was assigned as the charge transfer (CT) process of $Co^{2+} \rightarrow Co^{1+}$ attributed to electronic transfer between the O 2p and Co 3d orbitals [20]. These feature transitions are illustrated in the electronic band structure diagram shown in figure 5. Characteristic transitions denoted by (i), (ii) and (iii) correspond to the d–d transition of Co, the charge transfer gap and the band gap of the ZnO host lattice, respectively.

Figure 6 shows Raman spectra for all the samples using 488.0 nm as an excitation source. ZnO has C_{6v} symmetry and gives six Raman-active phonon modes in the first-order phonon spectrum at 101, 380, 408, 438, 574 and 583 cm^{-1} for the E_2(low), A_1(TO), E_1(TO), E_2(high), A_1(LO) and E_1(LO) phonon modes, respectively [21]. In addition the two-phonon signals at 332, 541 and 660 cm^{-1} are relatively strong [22]. A typical Raman spectrum of ZnO was observed for the undoped sample, on the other hand, three additional peaks originating from an impurity phase of Co_3O_4 were also observed at ∼490, ∼530 and ∼710 cm^{-1} for the sample of [Co] = 22.1% [28]. This shows good agreement with the XRD analysis. For the sample doped with Co, the E_2(high) phonon signal was considerably broadened with an increase in the Co doping level, as shown in the inset of figure 6. This is due to the 'alloying effect' [29], i.e. the compositional fluctuation caused by random substitution of Co into the Zn sites. Furthermore, an additional broad signal at 500–600 cm^{-1} appeared for the sample doped with Co. In previous research, an additional broad signal at 500–600 cm^{-1} has been commonly observed for doped or ion-implanted ZnO samples [23–26], and has been assigned as a defect-related signal induced by an O vacancy and lattice deterioration due to the impurity doping. However, this feature can not be explained solely as due to lattice deterioration caused by Co doping, because the XRD patterns showed the clear diffraction patterns corresponding to wurtzite ZnO structure, and the clear lattice fringe was also observed in the high-resolution TEM image. Here, figure 7 shows the Raman spectra for the sample of [Co] = 9.0% using different

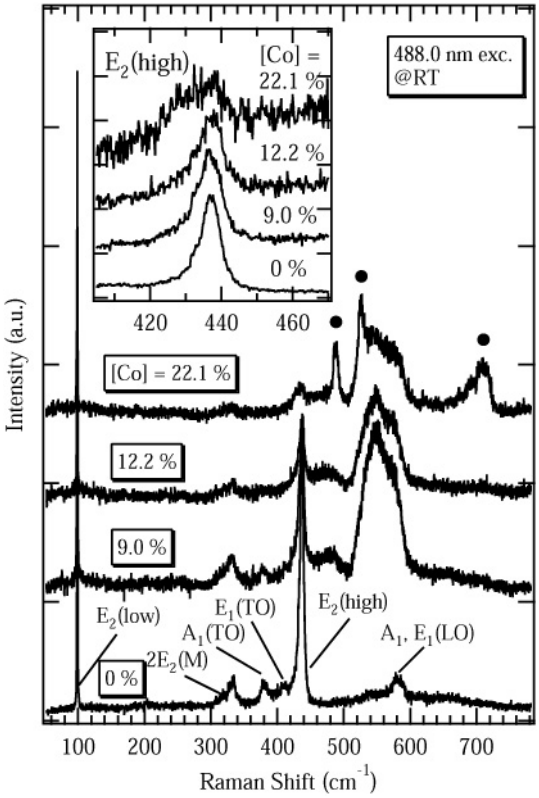

Figure 6. Raman spectra for the $Zn_{1-x}Co_xO$ samples using an Ar ion laser at 488.0 nm as an excitation source. Filled circles correspond to the Co_3O_4 secondary phase. The inset shows a close-up of E_2(high) phonon signal.

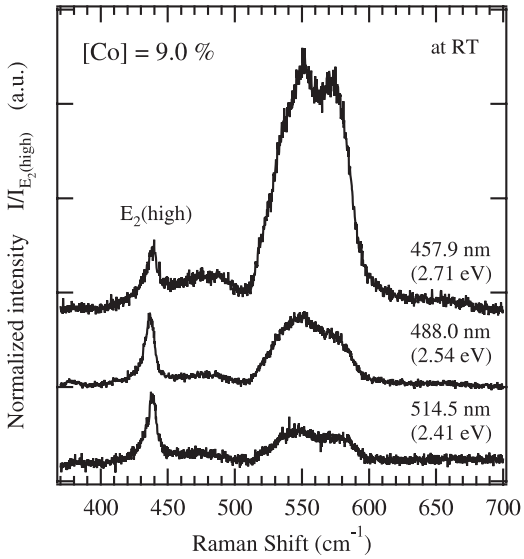

Figure 7. Raman spectra for the sample with [Co] = 9.0% excited by various wavelengths. Excitation wavelengths are denoted in the figure.

excitation wavelengths at 457.9 nm (2.71 eV), 488.0 nm (2.54 eV) and 514.5 nm (2.41 eV). Clear enhancement of the additional broad signal was observed with an increase in excitation photon energy. Recalling that a CT gap at 2.4–3.3 eV was observed for the Co-doped samples in optical absorption measurements, the additional broad signal rapidly increased in intensity as the excitation energy approached the CT gap energy. Therefore, this enhancement was interpreted as a resonant Raman process induced by the coupling with the LO phonon and photo-excited carriers mediated CT gap [27], indicating the possibility of photo-induced magnetism based on a double exchange interaction by visible light irradiation in ZnO doped with Co.

4. Conclusion

Structural and electronic properties of $Zn_{1-x}Co_xO$ crystals were studied using samples prepared by solid-state reaction method. Although the secondary phases such as Co_3O_4 and CoO were observed for the sample heavily doped with Co, the wurtzite ZnO crystal was well retained up to a Co composition of 22.1% and doped Co ions substituted into Zn sites of ZnO host lattice. XRD analysis showed that the *a*- and *c*-axis lengths increased and decreased, respectively, with an increase in Co composition. In optical absorption measurements, an additional absorption band appeared at 2.4–3.3 eV corresponding to a CT gap between the O 2p and Co 3d orbital. Furthermore, the Raman spectra showed clear enhancement of the LO phonon due to a resonant Raman effect caused by photo-excitation of the free carrier mediated CT gap. This result shows the generation of free carriers by visible light irradiation for Co-doped ZnO systems, indicating the possibility of photo-induced magnetism based on a double exchange interaction.

References

[1] Dietl T, Ohno H, Matsukura F, Cibért J and Ferrand D 2000 *Science* **287** 1019
[2] Sato K and Katayama-Yoshida H 2000 *Japan. J. Appl. Phys.* **39** L555
[3] Ueda K, Tabata H and Kawai T 2001 *Appl. Phys. Lett.* **79** 988
[4] Prellier W, Fouchet A, Mercey B, Simon Ch and Raveau B 2003 *Appl. Phys. Lett.* **82** 3490
[5] Yin Z, Chen N, Chai C and Yang F 2004 *J. Appl. Phys.* **96** 5093
[6] Zhou H, Hofmann D M, Hofstaetter A and Meyer B K 2003 *J. Appl. Phys.* **94** 1965
[7] Norberg N S, Kittilstved K R, Amonette J E, Kukkadapu R K, Schwartz D A and Gamelin D R 2003 *J. Am. Chem. Soc.* **126** 9387
[8] Deka S and Joy P A 2006 *Appl. Phys. Lett.* **89** 032508
[9] Cui J, Zeng Q and Gibson U J 2006 *J. Appl. Phys.* **99** 08M113
[10] Yang L W, Wu X L, Qiu T, Siu G G and Chu P K 2006 *J. Appl. Phys.* **99** 074303
[11] Quesada A, Garcia M A, Andrés M, Hernando A, Fernández J F, Caballero A C, Martin-González M S and Briones F 2006 *J. Appl. Phys.* **100** 113909
[12] Park J H, Kim M G, Jang H M, Ryu S and Kim Y M 2004 *Appl. Phys. Lett.* **84** 1338
[13] Luo J, Liang J K, Liu Q L, Liu F S, Zhang Y, Sun B J and Rao G H 2005 *J. Appl. Phys.* **97** 086106
[14] Martinez B, Sandiumenge F, Balcells Ll, Arbiol J, Sibieude F and Monty C 2005 *Phys. Rev.* B **72** 165202
[15] Martinez B, Sandiumenge F, Balcells Ll, Arbiol J, Sibieude F and Monty C 2005 *Appl. Phys. Lett.* **86** 103113
[16] Li W, Kang Q, Lin Z, Chu W, Chen D, Wu Z, Yan Y, Chen D and Huang F 2006 *Appl. Phys. Lett.* **89** 112507

[17] Sato K, Katayama-Yoshida H and Dederrichs P H 2005 *Japan. J. Appl. Phys.* **44** L948
[18] Jin Z, Fukumura T, Kawasaki M, Ando K, Saito H, Sekiguchi T, Yoo Y Z, Murakami M, Matsumoto Y, Hasegawa T and Koinuma H 2001 *Appl. Phys. Lett.* **78** 3824
[19] Koidl P 1977 *Phys. Rev.* B **15** 2493
[20] Malguth E, Hoffmann A and Phillips M R 2008 *Phys. Status Solidi* b **245** 455
[21] Damen T C, Porto S P S and Tell B 1966 *Phys. Rev.* **142** 570
[22] Calleja J M and Cardona M 1977 *Phys. Rev.* B **16** 3753
[23] Hasuike N, Fukumura H, Harima H, Kisoda K, Matsui H, Saeki H and Tabata H 2004 *J. Phys.: Condens. Matter* **16** S5807
[24] Reuss F, Kirchner C, Gruber Th, Kling R, Maschek S, Limmer W, Waag A and Ziemann P 2004 *J. Appl. Phys.* **96** 3385
[25] Samanta K, Dussan S, Katiyar R S and Bhattacharya P 2007 *Appl. Phys. Lett.* **90** 261903
[26] Hasuike N, Degyuchi R, Katoh H, Kisoda K, Nishio K, Isshiki T and Harima H 2007 *J. Phys.: Condens. Matter* **19** 365223
[27] Friedrich F and Nickel N H 2007 *Appl. Phys. Lett.* **91** 111903
[28] Hadjiev V G, Iliev M N and Vergilov I V 1988 *J. Phys. C: Solid State Phys.* **21** L199
[29] Davydov V Y, Goncharuk I N, Smirnov A N, Nikolaev A E, Lundin W V, Usikov A S, Klochikhin A A, Aderhold J, Graul J, Semchinova O and Harima H 2002 *Phys. Rev.* B **65** 125203